

# Influence of 3D particle shape on the mechanical behaviour through a novel characterization method

Noura Ouhbi<sup>1,3</sup>, Charles Voivret<sup>1</sup>, Guillaume Perrin<sup>2</sup>, and Jean-Noël Roux<sup>3</sup>

<sup>1</sup>Department of Lines, Tracks & Environment, Engineering & Projects, SNCF-Réseau, Saint-Denis, France

<sup>2</sup>CEA/DAM/DIF, Arpajon, France

<sup>3</sup>Université Paris-Est, Laboratoire Navier (UMR 8205), CNRS, ENPC, IFSTTAR, Marne-la-Vallée, France

**Abstract.** The sensitivity of the mechanical behaviour of railway ballast to particle shape variation is studied through Discrete Element Method (DEM) numerical simulations, focusing on some basic parameters such as solid fraction, coordination number, or force distribution. We present an innovative method to characterize 3D particle shape using Proper Orthogonal Decomposition (POD) of scanned ballast grains with a high accuracy. The method enables not only shape characterization but also the generation of 3D distinct and angular shapes. Algorithms are designed for face and edge recognition.

## 1 Introduction

In the last years, particle shape analysis has become a topic of interest in several fields. In railway engineering, the importance of grain size and shape for the behaviour of ballast (the granular layer made of centimetre sized, angular grains, supporting the tracks) has been highlighted in numerous experimental and numerical studies [1-4]. Connections between shape parameters and mechanical performance are however not well known. This is the issue addressed in the present study.

Such a research objective requires, given its complexity, some modelling of ballast shape, with various levels of accuracy. Powerful methods have been suggested to characterize shape (e.g spherical harmonics) [5, 6]. These methods, on attempting to reconstruct such shapes, fail to reproduce the “facetted” and “angular” aspect of the particles.

To overcome these limitations, we propose (Sec. 2.1) a method based on Proper Orthogonal Decomposition (POD) [7] apt to provide optimal descriptions of complex shapes. Particle generation is carried out (Sec.2.2) by a stochastic method called multivariate Kernel Density Estimation (KDE) [8], which proved successful in taking into account the high level of correlation between data on ballast grains. Finally, DEM simulations are used to assess the sensitivity of mechanical properties to particle shape.

## 2 Model

### 2.1 Shape characterization

Our study is based on 3D scans of 1000 ballast grains, with millimetre accuracy. The point clouds, cleaned

from possible outliers, first go through pre-processing steps which involve projecting onto a suitable common basis and aligning all grains according to their principal directions. A model reduction is then carried out through Proper Orthogonal Decomposition (POD) (commonly known as Principal Component Analysis in data analysis), a powerful tool to emphasize variation and bring out strong patterns in a dataset, thus easing data exploration and visualization. The POD method, as applied to ballast grain represented by magnitudes of radii in a chosen set of basis directions (as described in [9] in detail), does not assume any parametric description of grain shape but, rather, identifies appropriate basis functions by order of decreasing statistical relevance, thus capturing the dominant morphology features. Shape precision is controlled by choosing the size of the new reduced space representing data (Fig.1). A satisfactory convergence rate is obtained, in terms of morphology features, as the precision level increases [9]. One limitation, however, is the strong dependency of its efficiency on the sample size [10].

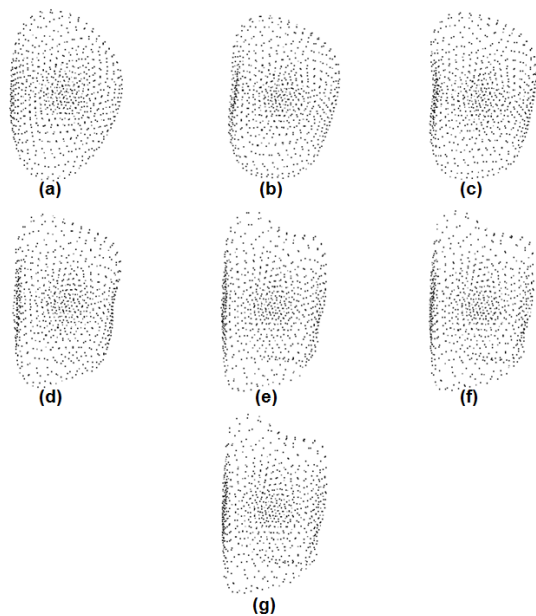
### 2.2 Complex shape generation

In order to increase the variability of shape in our numerical studies, we need a virtual grain generator. Basic parametric stochastic methods of generation applied to our grains [11] yield the right volume and surface area distributions, but fail to reproduce more advanced features such as angularity, faces, etc. Such features are statistically represented by the high-order correlations between points in space, which multivariate KDE, a non-parametric method proves apt to satisfactorily account for. An example of generated grains while keeping only 117 modes (99% of information) is presented in Fig. 2 and elongation

\* Corresponding author: noura.ouhbi@sncf.fr

distribution is shown in Fig. 3. We define elongation  $E$  using the three principal lengths of the grains  $S < I < L$ :  $E = \frac{I}{L}$ . We also compared surface area, volume, average radii, flatness ( $F = \frac{S}{I}$ ) and aspect ratio ( $AR = \frac{S}{L}$ ). The results we got in terms of likelihood values according to the Kolmogorov-Smirnov test were all above 0.8, which is a very satisfactory result.

After verifying these shape properties, we now present a new indicator which consists of faces/edges detection. The procedure for face detection is based on a clustering algorithm. After computing neighbours for each vertex, we use clustering algorithms to identify groups of neighbouring points with nearly parallel normal directions. Based on this clustering, we obtain groups that represent faces or edges. Using these clusters, we define curvature as the deviation of the vertices normal directions and thus we are able to distinct faces from edges in each grain. The distribution of the number of large faces and edge curvatures and an illustration are presented in Figs. 4 to 6. We chose to represent large faces as those that contain more than 100 points with parallel normal. This number was calibrated according to



the noticed number of large faces obtained on some examples of grains.

**Fig. 1.** Reconstructed grain with different precision levels (from (a) to (g): 80%; 85%; 90%; 95%; 99%; 99,9%; 100% of information on shape)

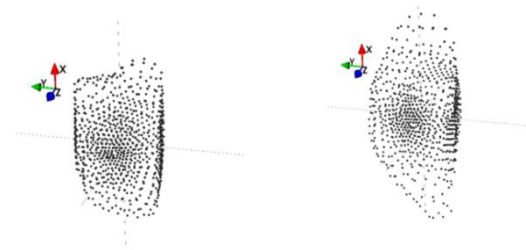


**Fig. 2.** Two generated ballast grains

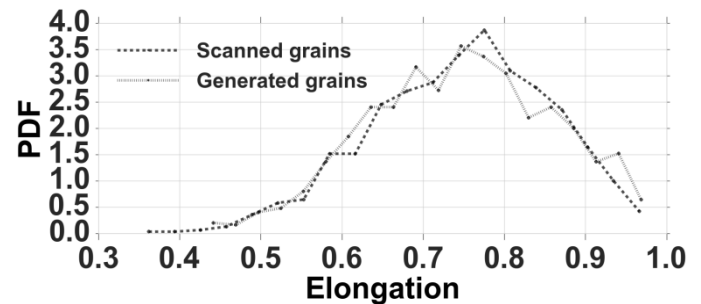


**Fig. 3.** Elongation Probability Function (PDF)

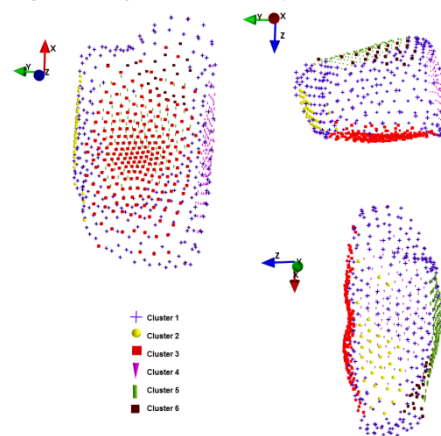


**Fig. 4.** Detection of faces for a generated ballast grain

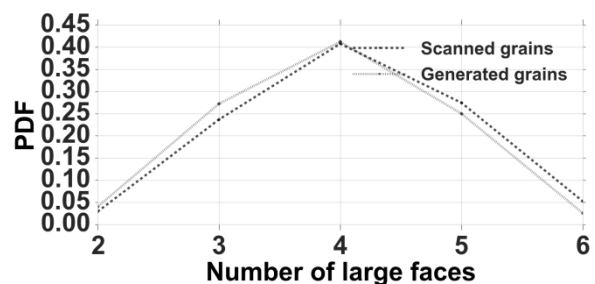


**Fig. 5.** Large faces (faces with number of points > 100 points) (PDF)

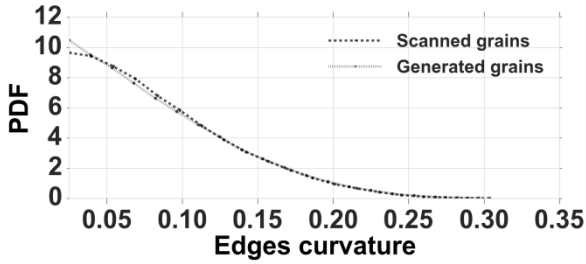


**Fig.6.** Edge curvature (Curvature = variation of normal directions; faces=low curvature, edges=High curvature) (PDF)

### 3 Numerical simulations

DEM simulations are carried out with LMG90 [12], a software apt to deal with rigid polyhedral grains. After a suitable meshing, grains are modeled as polyhedra. In a first stage, the shapes are further simplified as convex polyhedra, which enables much faster computations. This entails a loss of precision on shape (in the sense of Fig.1) of about 20% (which would be reduced to less than 5% with non-convex polyhedra). This restricts the relevance of simulations with large numbers of modes. Here we simulate an assembling procedure via one-dimensional compression between parallel planes with periodic lateral boundary conditions, without gravity. It is carried out using 300 grains, with 100 faces and 3 different shape precision levels after convex meshing: 30% (1 mode), 68% (11 modes) and 80% of information (800 modes). The sample is first generated by depositing the spheres circumscribed to the polyhedral (Fig. 7) in a cell with a constant square section ( $S = 30\text{ cm} \times 30\text{ cm}$ ). Three values of the intergranular friction coefficient  $\mu$  are compared: 0, 0.3 and 0.8. As a reference, a similar simulation is carried out with meshed spheres with 100 faces (and  $\mu=0.3$ ). Contacts with planes are frictionless. A constant force of  $F_0 = 500\text{ N}$  is applied to the upper mobile plane until an equilibrium state is approached, in which the contacts resist further compression (Fig.7). Figs. 8 to 11 show how the solid fraction  $\rho$  and the coordination numbers corresponding to simple (vertex-face or edge-edge), double (edge-face) and triple (face-face) contacts respectively denoted as  $z_1, z_2, z_3$  evolve in time towards their final equilibrium values. We note that the force supported by the bottom fixed plane converges to  $F_0$  after 3.8s. The ratio  $K = \frac{E_c}{\sigma D^3}$  of the kinetic energy per grain,  $E_c$ , to the characteristic energy scale  $\sigma D^3$  ( $\sigma$  denoting stress  $\frac{F_0}{S}$ , and  $D$  the average grain diameter) gradually decreases to  $4 \cdot 10^{-6}$  in 10 s. Such time scales are related to the initial state density and to grain and upper plane inertia.

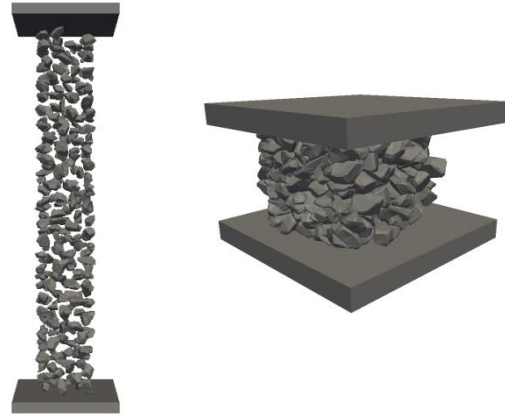


**Fig.7.** Assembling procedure: initial and final states.

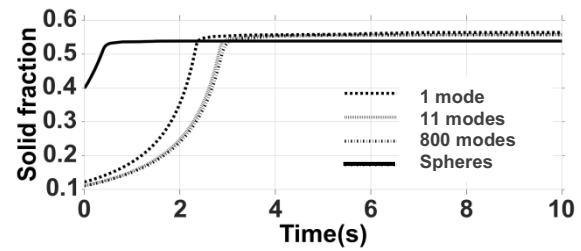


**Fig. 8.** Solid fraction vs time ( $\mu=0.3$ )

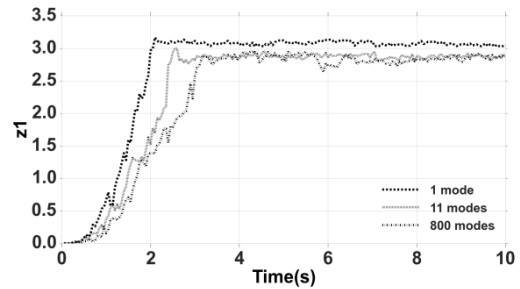


**Fig.9.**  $z_1$  vs time ( $\mu=0.3$ )

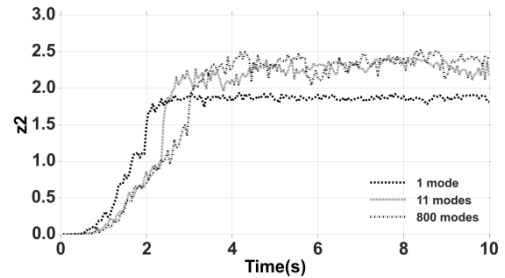


**Fig.10.**  $z_2$  vs time ( $\mu=0.3$ )

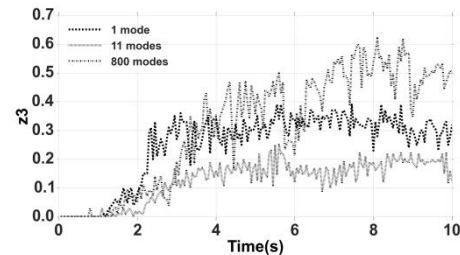


**Fig.11.**  $z_3$  vs time ( $\mu=0.3$ )

Final, equilibrium values of  $\rho, z_1, z_2, z_3$  are given in Table 1, along with those of  $x_0$ , the proportion of “rattlers” (grains carrying no force) for different numbers of modes and values of  $\mu$ .

**Table.1.** Evolution of some mechanical parameters

Parameter		$\rho$	$z_1$	$z_2$	$z_3$	$x_0$
N- $\mu$						
N	$\mu$					
11	0	0.690	4.360	3.766	0.320	0%
800	0	0.697	3.877	3.993	0.427	0%
1	0.3	0.590	3.046	1.206	0.213	7.6%
11	0.3	0.594	2.893	1.440	0.280	7.3%
800	0.3	0.602	2.874	1.593	0.332	5.08%
1	0.8	0.566	1.893	0.860	0.080	26.6%
11	0.8	0.567	1.886	0.980	0.080	26.33%
800	0.8	0.567	1.884	0.981	0.094	22.37%

We observe that the solid fraction increases with the number of modes, while  $z_1$  decreases and  $z_2$  and  $z_3$  increase. Grains with more accurate shape description tend to form slightly denser assemblies, with an increase of double and triple contacts, at the expense of simple ones. This shape effect is stronger for low friction coefficients. A strong increase of rattler fraction  $x_0$  should also be noted for growing  $\mu$ , as in spherical bead assemblies.

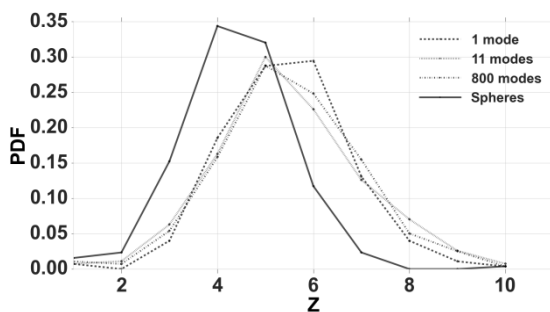


**Fig. 12.** Connectivity distribution ( $\mu=0.3$ ).

Fig.12 plots the distribution of connectivity  $Z$  (the fractions of grains having exactly  $Z$  contacting neighbours). A significant difference with spheres can be noted, while different shape models yield very similar results: Increasing the precision on shape modelling changes the type of contacts without affecting contact numbers.

## 4 Conclusions

The proposed new method to characterize the shape of ballast grains enables its description with controlled accuracy, and the generation of new sets of grains, similar to the real ones. Preliminary numerical simulations are carried out to quantify the impact of shape on mechanical properties, revealing that a very

significantly reduced number of parameters (11 shape functions) may be sufficient for our model. Beyond the simulated assembling stage for a solid granular packing, we expect the shear response to exhibit a higher sensitivity to shape, as observed in [13] for polyhedra with varying numbers of faces inscribed within the same sphere.

## Acknowledgements

The work has been supported by SNCF-Réseau Engineering and Projects, Lines Track & Environment Department.

## References

1. E. Azéma, Y. Descantes, N. Roquet, J. N. Roux, F. Chevoir. *Phys.Rev. E* **86**(3), (2012).
2. E. Azéma. Doctoral dissertation, Montpellier. (2007).
3. E. Azéma, F. Radjai, G. Saussine. *Mech. of Mat.* **41**(6), 729-741. (2009).
4. J. C. Quezada, P. Breul, G. Saussine, F. Radjai. *Comp. and Geotech.* **55**, 248-253. (2014).
5. G. Mollon, J. Zhao. *Gran. Mat.* **15**(1), 95-108. (2013).
6. M. Grigoriu, E. Garboczi, C. Kafali. *Powd. Tech.* **166**(3), 123-138. (2006).
7. Y. C. Liang, H. P. Lee, S. P. Lim, W. Z. Lin, K. H. Lee, C. G. Wu. *Jour. of Sou. and vibr.* **252**(3), 527-544. (2002).
8. D. W. Scott, S. R. Sain. *Handbook of Statistics.* **V24**, 229-261. (2005).
9. N. Ouhbi, C. Voivret, G. Perrin, J. N. Roux. *Procedia Engineering*, **143**, 1120-1127. (2016).
10. N. Ouhbi, C. Voivret, G. Perrin, J.N. Roux. *Proceedings of the 3rd International Conference on Particle-based Methods, held in Barcelona, Spain*, pp. 545–557. (2015).
11. G. Perrin, C. Soize, N. Ouhbi. Submitted to *Journal of Comp. Stat. & Data An.* (2016).
12. F. Dubois, F., M. Jean, M. Renouf, et al. *LMGC90. 10e colloque national en calcul des structures. Giens, France.* (2011)
13. E. Azéma, F. Radjai, F. Dubois. *Phys. Rev. E* **87**. (2013).